

Pharmaceutical Research Institute¹, China Pharmaceutical University; State Key Laboratory of Bioelectronics², Jiangsu Laboratory for Biomaterials and Devices, School of Biological Science and Medical Engineering, Southeast University, Nanjing, China

Characterization and *in vitro* cellular uptake of PEG coated iron oxide nanoparticles as MRI contrast agent

Y. J. CHEN^{1,2}, J. TAO^{1,2}, F. XIONG², J. B. ZHU¹, N. GU², K. K. GENG^{1,2}

Received November 21, 2009, accepted November 30, 2009

Jia Bi Zhu, Pharmaceutical Research Institute, China Pharmaceutical University, 24 Tongjiaxiang, Nanjing 210009, China
Zhu_Jiabi@163.com

Ning Gu, State Key Laboratory of Bioelectronics, Jiangsu Laboratory for Biomaterials and Devices, School of Biological Science and Medical Engineering, Southeast University, Nanjing 210009, China
Guning@seu.edu.cn

Pharmazie 65: 481–486 (2010)

doi: 10.1691/ph.2010.9372

Monodisperse magnetic iron oxide nanoparticles (MNPs), coated with PEG at different molecular weight, were prepared via self-assembly method. The particle diameters were measured by dynamic light scattering and transmission electron microscope. Increasing the molecular weight of PEG in the coating polymer increased the overall particles diameter. As coating thickness increased, the saturation magnetization (M_s) and T_2 relaxivity decreased. The interactions of these MNPs with macrophage cells were also investigated. The results showed that cellular uptakes of MNPs depended on nanoparticle concentration and surface chemistry. The results of this study will have implications on the chemical design of nanomaterials for bio-imaging and bio-detection.

1. Introduction

Magnetic iron oxide nanoparticles (MNPs) are of considerable interest in various biomedical applications, such as magnetic resonance imaging (MRI) contrast enhancement (Seo et al. 2006; Cheng et al. 2005; Tomita et al. 2008), hyperthermia (Sonvico et al. 2005), targeted drug delivery (Talelli et al. 2009; Tai et al. 2009) and cell separation (Horak et al. 2007), due to their size-dependent superparamagnetism, low toxicity and biocompatibility with cells and tissues (Mahmoudi et al. 2009). Iron oxide nanoparticles may potentially provide higher contrast enhancement in MRI than conventional paramagnetic Gd-based contrast agents (Aime et al. 2002) because of their superparamagnetic property. Moreover, MNPs with suitable particle size can specifically accumulate in tumor sites by EPR effect as a result of the presence of leaky vasculatures around solid tumors (Matsumura et al. 1986).

Nanoparticle size (Muller et al. 2007; Chithrani et al. 2006), surface chemistry (hydrophilicity/hydrophobicity) (Yuan et al. 2006), charge (Win et al. 2005) and their interactions with the components of the reticuloendothelial system (RES) (Owen et al. 2006) have a profound effect on the biodistribution of nanoparticles. Therefore, surface modification of iron oxide nanoparticles with biocompatible polymers is potentially beneficial to prepare MR contrast agents for *in vivo* applications such as cancer imaging (Larsen et al. 2009; Barrera et al. 2009). In particular, a protein resistant surface is required for the nanoparticles to accumulate in tumors by the enhanced permeability and retention (EPR) effect during systemic circulation. Otherwise, nanoparticles are quickly cleared by RES due to its high surface-to-volume ratio as well as attractive forces between the

nanoparticles (Herrwerth et al. 2003). Several synthetic and natural polymers such as dextran (Jarrett et al. 2007), polyethylene glycol (PEG) (Larsen et al. 2009), or polyethylene oxide (PEO) (Narain et al. 2007), have been employed to modify the surface of the particles to minimize aggregation of the particles. In the commonly used method, the polymer is covalently linked to the surface of iron oxide cores, which requires developing complex conjugation chemistry and is impractical to synthesize in large amounts on an industrial scale. In another approach, iron oxide cores are dispersed in polymers (e.g., poly-DL-lactide-co-glycolide (PLGA) (Okassa et al. 2007), polylactide (PLL) (Arbab et al. 2003) that are typically used in developing other nanocarriers for drug delivery. However, this approach usually leads to the formation of large-sized microparticles with limited encapsulation of MNPs resulting in significant loss in magnetization (~40–50%) of the iron oxide cores (Strable et al. 2001), which could adversely influence its imaging property including magnetic spin anisotropy (spin disorders) and ultimately proton relaxivity (Duan et al. 2008). Therefore, the use of magnetic nanoparticles for cancer imaging must address issues such as stability in physiology environment in terms of evasion from agglomeration and macrophage uptake, retention of magnetic properties and high contrast enhancement after modification with polymers. And to the best of our knowledge, not much work has been done regarding to *in vivo* application and non-invasive cancer imaging.

We have previously developed an antibiofouling of PEG coated monodisperse iron oxide nanoparticles comprising a “surface anchoring moiety” (oleic acid) and a “protein-resistant moiety” (PEG), denoted as methoxy-poly(ethylene glycol)-lipids with di-oleoyl chains (DO-PEG), which is synthesized from

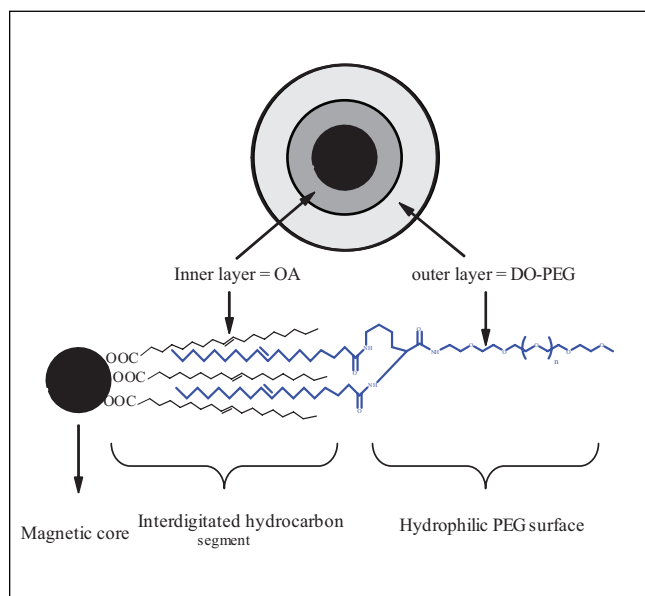


Fig. 1: Schematic structure of PEG coated iron oxide nanoparticles

N^{α},N^{ϵ} -dioxyl lysine and Amino-mPEG with various molecular weight (MW = 1000, 2000, 4000). Protein and cell resistant surfaces are successfully generated on oleic acid capped iron oxide cores via the interactions between the inner oleic acid layer and the hydrophobic groups of outer DO-PEG polymer (Fig. 1). And the resulting particles have been demonstrated retention of magnetic properties and high contrast enhancement after modification with polymers, and much reduced non-specific uptake by macrophage cells. These make the particles ideal candidates for higher signal-to-noise ratio in cancer imaging. Work on using these particles for cancer imaging is underway.

2. Investigations, results and discussion

2.1. Synthesis, self-assembly and characterization of PEG coated magnetic nanoparticles

Monodisperse magnetite nanoparticles were synthesized by thermal decomposition of iron-oleate in the presence of oleic

acid. The first advantage of this procedure based on iron-oleate decomposition was that highly crystalline and monodisperse iron oxide NPs could be prepared in a wide range of sizes (from 6 to 30 nm) merely by varying the rate of heating, the reaction temperature of the solvent (usually exceeded the boiling temperature of the solvent). The second one was that iron-oleate was inexpensive and non-toxic. The TEM image (Fig. 2A) showed that nanoparticles were monodisperse and the core particle size was about 10 nm. These nanoparticles were highly crystalline and uniform but were not soluble in water due to the hydrophobic oleic acid capping layer.

To transfer hydrophobic oleic acid coated magnetic cores from organic to aqueous, the hydrophobic cores were encapsulated within an amphiphilic polymer layer (DO-PEG), which was consisted of hydrophobic N^{α},N^{ϵ} -dioxyl lysine and hydrophilic methyl-polyoxyethylene amine and was condensed via EDC/DMAP chemistry. An interesting feature was that the PEG coated nanoparticles had a hydrophilic layer due to the interactions between the inner oleic acid and the hydrophobic groups of the outer polymer. In the PEGylated bilayer system, the outer PEG segment provided steric stabilization and water dispersibility to the superparamagnetic nanoparticles. In order to study the effect of PEG length on magnetic properties and reducing non-specific uptake, a series of DO-PEG polymers with PEG molecular weight being 1000, 2000, 4000 were used to encapsulate the magnetic cores. After modification, the nanoparticles were able to disperse in water, forming a clear solution. Fig. 2B showed TEM image of the iron oxide nanoparticles coated by DO-PEG₂₀₀₀. Comparing Fig. 2A and B, one could see that there was no obvious change in core size after surface modification with DO-PEG. The PEG coating thickness around the nanoparticles was characterized with dynamic light scattering (DLS) which measured the hydrodynamic diameter of the nanoparticles in their dispersion state. The mean hydrodynamic size of nanoparticles (measured in distilled water) was about 42.5 ± 3.3 nm, 57.0 ± 2.8 nm and 77.0 ± 5.4 nm for PEG₁₀₀₀, PEG₂₀₀₀ and PEG₄₀₀₀ coated nanoparticles, respectively, indicating magnetic cores were successfully encapsulated in the hydrophobic core of DO-PEG.

The magnetic property of MNPs was measured by VSM. A typical plot of magnetization versus applied magnetic field (M-H loop) is shown in Fig. 3 which provided evidence that all the MNPs were superparamagnetic at room temperature, with no hysteresis and perfect Langevin behavior (Chantrell 1978).

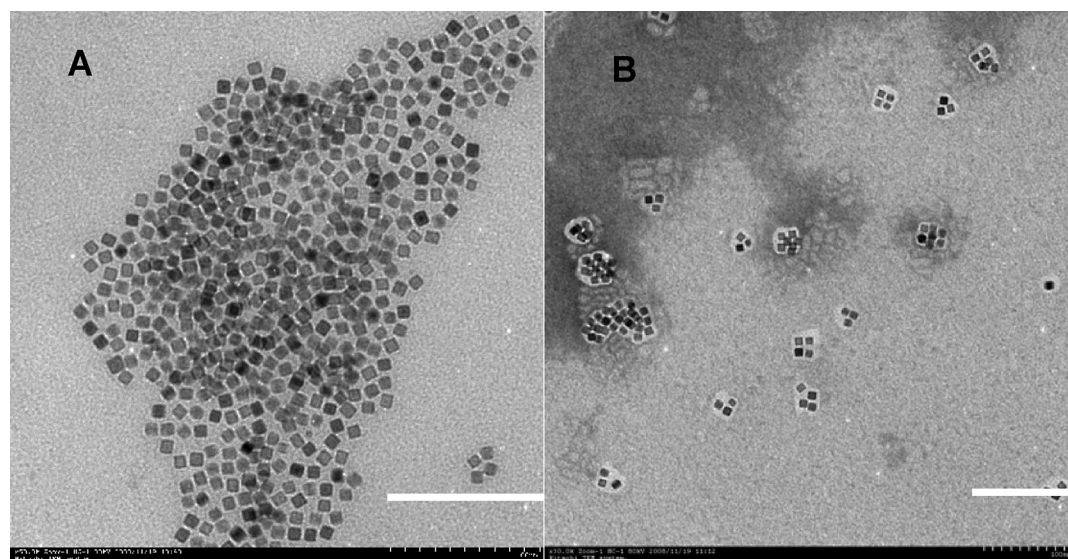


Fig. 2: Transmission electron microscopy images of (A) oleic acid coated magnetic nanoparticles (MNPs-OA) dispersed in hexane; (B) PEG coated magnetic nanoparticles (MNPs-PEG₂₀₀₀). The bar represents 100 nm

Therefore the superparamagnetic property would not be altered after the coating process. The magnetic parameters such as saturation magnetization (M_s), coercivity (H_c) and remnant magnetization (M_r) were given in the Table. The M_s of oleic acid, PEG₁₀₀₀, PEG₂₀₀₀ and PEG₄₀₀₀ coated nanoparticles were determined to be 82.7, 71.1, 60.7, 47.9 emu/g Fe, respectively. There were several approaches that could explain the reduction of M_s for polymer coated magnetic nanoparticles (Popplewell et al. 1995; Mikhayaylvo et al. 2004). In this case, the presence of nonmagnetic surfactant molecules on the surface of oleic acid coated magnetic nanoparticles led to decrease of the M_s .

2.2. Magnetic resonance imaging characteristics of PEG coated magnetic nanoparticles

Effective magnetic resonance (MR) contrast agents must have a strong effect to accelerate spin-lattice relaxation (T_1), which produced bright or positive contrast images, or to shorten spin-spin relaxation (T_2), which produced dark or negative-contrast images (Tapan et al. 2008). Iron oxides were effective MR agents because of their high relaxivities and a high capacity to achieve T_2 relaxation. The T_2 relaxation process occurred due to the exchange of energy between protons in water molecules. In the presence of an externally applied magnetic field, inhomogeneity in the magnetic field was created by magnetic nanoparticles which resulted in dephasing of the magnetic moments of protons and hence T_2 shortening. This effect was quantified in the concentration-independent transverse relaxivity r_2 , that was, the ability of the contrast agent to shorten T_2 . The MRI signal intensity of nanoparticles decreased in varied degrees in T_2 -weighted imaging depending on the Fe concentration in agarose solution. As the nanoparticles concentration, measured in $\mu\text{g Fe/mL}$, was increased in the agarose solution, the signal intensity decreased (Fig. 4). The relaxation rate, $R_2 = 1/T_2$, was linearly proportional to the iron concentration (Fig. 4). We also found T_2 relaxivity in the following order of decreasing values: MNPs-PEG₁₀₀₀ > MNPs-PEG₂₀₀₀ > MNPs-PEG₄₀₀₀ (Fig. 5). The r_2 value of MNPs-PEG₁₀₀₀ was about 1.5 times greater than that of the MNPs-PEG₂₀₀₀ and MNPs-PEG₄₀₀₀ ($p < 0.05$). But no significant variation between MNPs-PEG₂₀₀₀ and MNPs-PEG₄₀₀₀ was observed ($p > 0.05$). These results indicated that the r_2 value decreased as the molecular weight of DO-PEG polymer and thus as the MNPs diameter increased. T_2 relaxation process required close proximity of hydrogen atoms to the contrast agent (Okuhata et al. 1999). As indicated by the results, coating thickness played important role in determining the net relaxivity of MNPs, which was consistent with previous observation (Lacoste et al. 2007).

2.3. In vitro cell cytotoxicity study and cell uptake

The potential toxicity of PEG coated iron oxide nanoparticles as a MR contrast agent was demonstrated by the MTT cyto-

Table: Magnetic properties of oleic acid, PEG coated superparamagnetic nanoparticles

Samples	M_s (emu/g)	H_c (Oe)	M_r (emu/g)
MNPs-OA	82.7 ± 4.2	4.6 ± 0.8	0.4 ± 0.05
MNPs-PEG ₁₀₀₀	71.1 ± 3.1	3.5 ± 0.6	0.4 ± 0.08
MNPs-PEG ₂₀₀₀	$60.7 \pm 3.4^*$	4.2 ± 0.8	0.5 ± 0.03
MNPs-PEG ₄₀₀₀	$47.9 \pm 2.8^*$	2.8 ± 0.3	0.3 ± 0.03

Results were given as mean \pm S.D. (n = 4)

* $P < 0.05$ vs. MNPs-OA

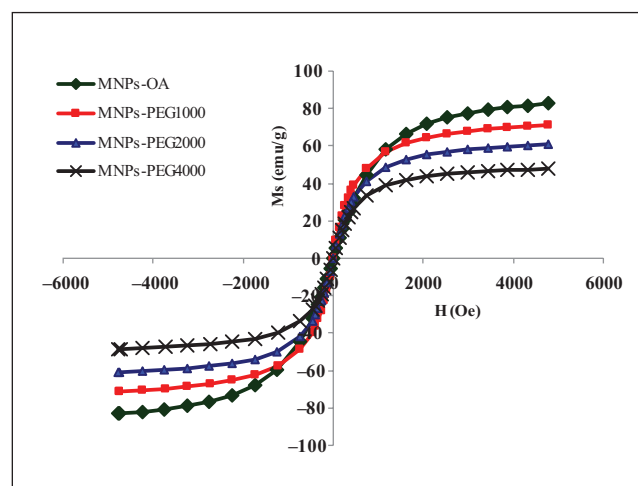


Fig. 3: Hysteresis loops at room temperature for MNPs-OA, MNPs-PEG₁₀₀₀, MNPs-PEG₂₀₀₀ and MNPs-PEG₄₀₀₀

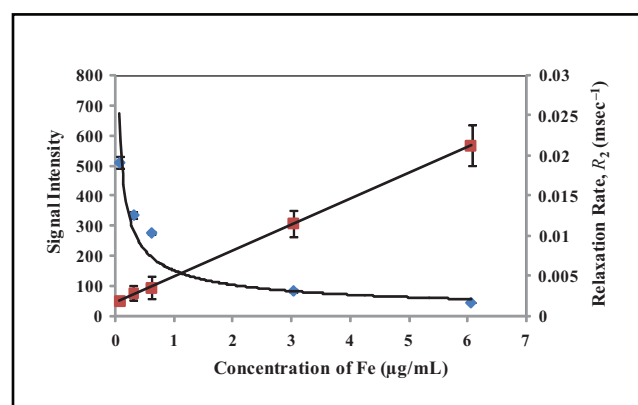


Fig. 4: Magnetic resonance imaging properties of MNPs-PEG₂₀₀₀: signal intensity of T_2 relaxation time (TR = 3500 ms, TE = 100 ms) at different iron concentration and T_2 relaxation rate (R_2) of MNPs vs. iron concentration

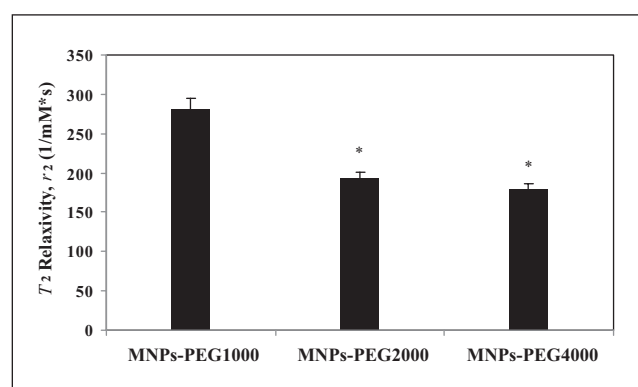


Fig. 5: Effect of coating thickness on magnetic imaging properties: comparison of T_2 relaxivity (r_2) of different formulation of MNPs. Results were given as mean \pm S.D. (n = 4), * $p < 0.05$ vs. MNPs-PEG₁₀₀₀

toxicity assay. After 12 h, cell viability was examined. Fig. 6 showed these nanoparticles did not inhibit KB cells growth with up to 0.2 mg Fe/mL. These results indicated that PEG coated nanoparticles expressed low cytotoxicity even at relatively high concentration. Since the amount of iron at the highest concentration (0.2 mg Fe/mL) far exceeded that of iron used in conventional iron oxide nanoparticles based MR contrast agent for mice (1–20 mg/kg), the PEG coated nanoparticles could be used as safe MR contrast agent.

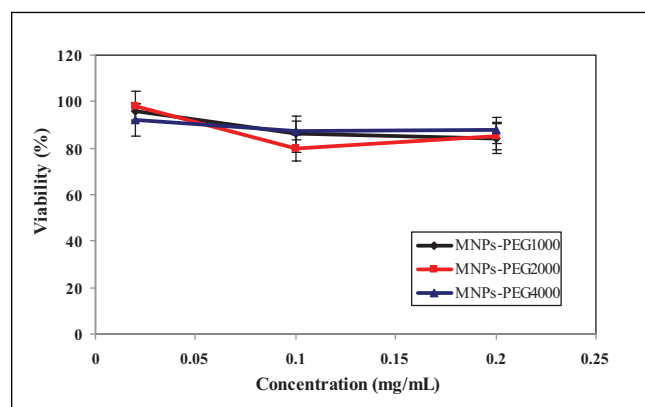


Fig. 6: *In vitro* cell viability graphs of MNPs-PEG₁₀₀₀, MNPs-PEG₂₀₀₀ and MNPs-PEG₄₀₀₀ as a function of different iron concentrations of 0.02, 0.1 and 0.2 mg/10⁴ cells by MTT. Percent viability of cells was expressed relative to control cells. Results were shown as mean \pm SD (n = 4)

The key for *in vivo* use of iron oxide nanoparticles as a contrast agent for cancer imaging was lower uptake of nanoparticles by reticular endothelial system (RES) such as macrophages (Cheng et al. 2005). Therefore the iron oxide nanoparticles could circulate long enough to be accumulated into tumor by the EPR effect. To investigate this hypothesis *in vitro* cell uptake experiments were carried out using a macrophage cell line RAW264.7. The uptake of various concentrations of MNPs-PEG₁₀₀₀, MNPs-PEG₂₀₀₀, MNPs-PEG₄₀₀₀ by macrophages were compared with that of Feridex I.V., which was currently used clinically for MRI and was known to be taken up by macrophages because of its size being larger than 100 nm (Lee et al. 2006). Uptake of nanoparticles was concentration-dependent, with dosing concentration increasing from 0.02 mg Fe/mL to 0.1 mg Fe/mL. The uptake amount was enhanced 2.5–4-fold, which was consistent with previous observations (Xie et al. 2007; Mosqueira et al. 1999). Fig. 7 showed the macrophage uptake results at the 0.04 mg Fe/mL of PEG coated samples. It could be seen that the dextran coated nanoparticles gave the highest uptake, followed by PEG₁₀₀₀ coated particles, of which the uptake was about 30% of that from dextran coated ones ($p < 0.05$). The uptake ratios of PEG₂₀₀₀ and PEG₄₀₀₀ coated particles to dextran coated ones decreased to about 15% ($p < 0.05$). Moreover, the uptake of PEG₂₀₀₀ and PEG₄₀₀₀ coated particles were considerably lower than that coated with PEG₁₀₀₀, but no significant variation was observed ($p > 0.05$). PEG with molecular weight higher than 2000 gave dense coating over the surface of the nanoparticles, and therefore the length of PEG chain became insignificant factor in terms of non-specific uptake.

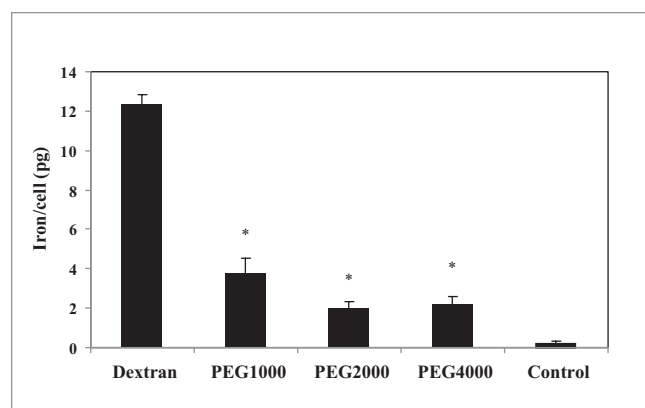


Fig. 7: Determination of the various MNPs for interaction with macrophage cells with initial concentration at 0.04 mg Fe/mL. The cells were incubated with MNPs for 6 h. Results were shown as mean \pm SD (n = 4), * $p < 0.05$ vs. MNPs-Dextran

3. Experimental

3.1. Materials

Methoxy-poly(ethylene glycol)-lipids with di-oleoyl chains (DO-PEG) was synthesized according to our previous work with slight modification (Xiong et al. 2006). 1-Octadecene was purchased from Alfa Aesar. PRMI-1640 was purchased from Gibco. The other chemicals were analytical reagents and purchased from Shanghai Chemical Reagent Corporation, China. All chemicals were used as received.

3.2. Synthesis of monodisperse iron oxide nanoparticles coated with oleic acid

Monodisperse oleic acid-capped iron oxide nanoparticles of 10 nm in diameter were synthesized in organic solvent at high temperature as reported previously (Park et al. 2004). First, iron-oleate complex was prepared by reacting metal chlorides and sodium oleate. In a typical experiment, 1.08 g of iron chloride and 3.65 g of sodium oleate were dissolved in a mixture solvent composed of 8 mL ethanol, 6 mL distilled water and 14 mL hexane. And then, the solution was heated to 70 °C under magnetic stirring conditions and kept at that temperature for 4 h. The upper organic layer containing the iron-oleate complex was washed with 5 mL of distilled water. After evaporating hexane, the iron-oleate complex in a waxy solid form was obtained.

Second, 3.6 g of iron-oleate complex and 0.57 g of oleic acid were dissolved in 20 g of 1-octadecene. The reaction mixture was heated to 320 °C at a constant heating rate of 3.3 °C/min under a nitrogen atmosphere, and then kept at that temperature for 30 min. The resulting solution was cooled and precipitated by addition of excess ethanol and centrifugation. The precipitate containing oleic acid coated magnetite nanoparticles was washed 4–5 times with ethanol.

3.3. Surface modification of oleic acid coated iron oxide nanoparticles with DO-PEG

Three amphiphilic DO-PEG polymers modified iron oxide nanoparticles with 1000, 2000 and 4000 Da molecular weight of PEG chains were prepared via the self-assembly method. Briefly, DO-PEG (60 μ mol) and oleic acid-coated magnetite nanoparticles (10 mg) were dissolved in THF (2 mL). The above solution was slowly added into 5 mL of deionized water under sonication using an ultrasonic generator (KQ116, Ultrasonic Instrument Co., Ltd., Kunshan, China) and then dialyzed against deionized water for 2 days to allow the formation of hydrophilic nanoparticles and to remove organic solvents (Mw cut-off: 50,000 Da). Afterwards, the nanoparticles solution was removed from the dialysis bag and filtered through a 0.22 μ m membrane to remove large aggregates. Then, DO-PEG coated nanoparticles were separated by magnetic decantation with a permanent magnet.

3.4. Characterization of magnetic nanoparticles

The hydrodynamic size distribution data of MNPs were measured with a photon correlation spectrometer light scattering apparatus zeta potential/particle sizer 3000HS (Malvern Instruments, UK) and analyzed by the Zetasizer 3000H (MALVERN software). TEM observations were photographed with an H-7650 transmission electron microscope (Hitachi, Japan) at an acceleration voltage of 100 kV. The samples were dropped onto a carbon-coated copper grid, forming a thin liquid film. The films on the grid were negatively stained by adding immediately a drop of 2 wt. % phosphotungstic acid and then air dried. The magnetic measurements were carried out with a Vibrating Sample Magnetometer (VSM, Lakeshore 7407).

3.5. Magnetic resonance imaging

Suspensions of MNPs were prepared in 2% agarose solution and scanned under a clinical 1.5 T MR imager (Eclipse, Philips Medical Systems, The Netherlands) by using a 12.7-cm receive-only surface coil at room temperature. T_2 -weighted images were acquired using the following parameters: TR/TE, 3500/100 ms; DFOV, 4.5 \times 4.5 mm; matrix, 256 \times 256; slice thickness, 1 mm. The magnitudes of image intensities were measured within manually-drawn regions of interest (ROIs) for each of the samples. Relaxation rates R_2 ($R_2 = 1/T_2$) were calculated with different iron concentrations. T_2 relaxivity rate (r_2) was then calculated as slope from a plot R_2 vs. iron concentration in agarose solution.

3.6. Cell culture

Oral Squamous Carcinoma Cell line KB and macrophage cell line RAW 264.7 were purchased from the Institute of Biochemistry and Cell Biology, Shanghai Institute of Biological Sciences, Chinese Academy of Sciences (Shanghai, China). Cells were cultured in RPMI 1640 medium containing

10% fetal calf serum (FCS), 100 IU/mL penicillin and 100 IU/mL streptomycin and incubated at 37 °C in 5% CO₂ atmosphere. Medium was replaced every other day. For control experiments, medium having no nanoparticle was used. Each cell was detached mechanically and adjusted to the required concentration of viable cells, by counting in a hemocytometer in the presence of trypan blue.

3.7. *In vitro* cell cytotoxicity studies

The KB cell line was used to measure the *in vitro* cell cytotoxicity of iron oxide nanoparticles coated with different PEG's in medium. An amount of 10⁴ cells of KB were plated in each well of a 96-well plate. After 24 h of culture, the medium in the wells was replaced with the fresh medium containing nanoparticles in concentration range 0–0.2 mg Fe mL⁻¹. After 12 h of incubation, the supernatant was removed and cells were washed three times with PBS (pH 7.4). Then, 100 µL of MTT solution was added to each well. After incubation for 4 h at 37 °C, each well was treated with 100 µL of DMSO with pipetting for 3 to 5 min. Absorbance of the solution at 570 nm was measured by a microplate reader (Model 680, Bio-RAD). The spectrophotometer was calibrated to zero absorbance, using culture medium without cells. The relative cell viability (%) related to control wells containing cell culture medium without nanoparticles was calculated by $[A]_{\text{test}}/[A]_{\text{control}} \times 100$. Where $[A]_{\text{test}}$ is the absorbance of the test sample and $[A]_{\text{control}}$ is the absorbance of control sample.

3.8. Nanoparticle uptake by macrophages

An amount of 10⁵ cells of Raw 264.7 macrophages were seeded in each well of a 24-well plate. After incubation of 24 h, the medium was removed. The cells were washed three times with PBS (pH 7.4) before iron oxide nanoparticles coated with different PEG's and Feridex I.V. diluted in RPMI, each with different concentrations (0.02, 0.04, 0.10 mg Fe mL⁻¹) were added. Cells grown without any nanoparticles were used as control. After 6 h, the cell layer was treated with a 2 h digestion of particles in 30% v/v HCl at 60 °C. A total of 1.0 mg of potassic persulphate was added to oxidize the ferrous ions present in the above solution to ferric ions. Then, 1.0 ml of 0.1 M solution of potassium thiocyanate was added to this solution to form the iron-thiocyanate complex. 150 µL of the mixture was transferred to a 96-well plate and the absorbance was measured after 10 min at 480 nm using a microplate reader (Model 680, Bio-RAD) (Ge et al. 2009). A standard curve for iron was made under identical conditions using known amount of FeCl₃·6H₂O solution.

Acknowledgements: This work was partly supported by “211 project” and “985 project” university grant from Southeast University awarded to Dr. Xiong Fei (Nos. 4007031040 and 9207032444), National Basic Research Program of China (Nos. 2006CB933206), and National Natural Science Foundation of China (Nos. 60725101, 30870689, 30970754 and 20903021).

References

- Aime S, Cabella C, Colombatto S, Crich SG, Ginolio E (2002) Insights into the use of paramagnetic Gd(III) complexes in MR-molecular imaging investigations. *J Magn Reson Imaging* 16: 394–406.
- Arbab AS, Bashaw LA, Miller BR, Jordan EK (2003) Characterization of biophysical and metabolic properties of cells labeled with superparamagnetic iron oxide nanoparticles and transfection agent for cellular MR imaging. *Radiology* 229: 838–846.
- Barrera C, Herrera AP, Rinaldi C (2009) Colloidal dispersions of monodisperse magnetite nanoparticles modified with poly(ethylene glycol). *J Colloid Interface Sci* 329: 107–113.
- Chantrell RW, Popplewell J, Charles SW (1978) Measurements of particle size distribution parameters in ferrofluids. *IEEE Trans Magn* 14: 975–977.
- Cheng FY, Su CH, Yang YS, Yeh CS, Tsai CY (2005) Characterization of aqueous dispersions of Fe₃O₄ nanoparticles and their biomedical applications. *Biomaterials* 26: 729–738.
- Chithrani BD, Ghazani AA, Chan WW (2006) Determining the Size and Shape Dependence of Gold Nanoparticle Uptake into Mammalian Cells. *Nano Lett* 6: 662–668.
- Duan HW, Kuang M, Wang XX (2008) Reexamining the effect of particles size and surface chemistry on the magnetic properties of iron oxide nanocrystals: new insights into spin disorder and proton relaxivity. *J Phys Chem C* 112: 8127–8131.
- Ge Y, Zhang Y, Gu N (2009) Effect of surface charge and agglomerate degree of magnetic iron oxide nanoparticles on KB cellular uptake *in vitro*. *Colloids Surf B* 73: 294–301.
- Herrwerth S, Eck W, Reinhardt S, Grunze M (2003) Factors that determine the protein resistance of oligoether self-assembled monolayers – internal

- hydrophilicity, terminal hydrophilicity, and lateral packing density. *J Am Chem Soc* 125: 9359–9366.
- Horak D, Babic M, Jendelová P, Herynek V, Trchová M (2007) D-mannose-modified iron oxide nanoparticles for stem cell labeling. *Bioconjug Chem* 18: 635–644.
- Jarrett BR, Frendo M, Vogan J (2007) Size-controlled synthesis of dextran sulfate coated iron oxide nanoparticles for magnetic resonance imaging. *Nanotechnology* 18: 35603–35610.
- Lacoste L, Nitin N, Zurkiya O (2007) Coating thickness of magnetic iron oxide nanoparticles affects r2 relaxivity. *J Magn Reson Imaging* 26: 1634–1641.
- Larsen EK, Nielsen T, Wittenborn T, Birkedal H (2009) Size-dependent accumulation of PEGylated silane-coated magnetic iron oxide nanoparticles in murine tumors. *ACS Nano* 3: 1947–1951.
- Lee H, Lee E, Kim DK, Jang NK (2006) Antibiofouling polymer-coated superparamagnetic iron oxide nanoparticles as potential magnetic resonance contrast agents for *in vivo* cancer imaging. *J Am Chem Soc* 128: 7383–7389.
- Mahmoudi M, Simchi A, Milani AS, Stroeve P (2009) Cell toxicity of superparamagnetic iron oxide nanoparticles. *J Colloid Interface Sci* 336: 510–518.
- Matsumura Y, Maeda H (1986) A new concept for macromolecular therapeutics in cancer chemotherapy: mechanism of tumorotropic accumulation of proteins and the antitumor agent smancs. *Cancer Res* 46: 6387–6392.
- Mikhayaylo M, Kim DK, Berry CC (2004) BSA immobilization on amine-functionalized superparamagnetic iron oxide nanoparticles. *Chem Mater* 16: 2344–2354.
- Mosqueira VCF, Legrand P, Gref R (1999) Interactions between a macrophage cell line (J774A1) and surface-modified poly(D,L-lactide) nanocapsules bearing poly(ethylene glycol). *J Drug Target* 7: 65–78.
- Muller K, Skeppera JN, Posfai M, Trivedi R (2007) Effect of ultrasmall superparamagnetic iron oxide nanoparticles (Ferumoxtran-10) on human monocyte-macrophages *in vitro*. *Biomaterials* 28: 1629–1642.
- Narain R, Gonzales M, Hoffman AS, Stayton PS, Krishnan KM (2007) Synthesis of monodisperse biotinylated p(NIPAAm)-coated iron oxide magnetic nanoparticles and their bioconjugation to streptavidin. *Langmuir* 23: 6299–6304.
- Okassa LN, Marchais H, Douziech-Eyrolles L (2007) Optimization of iron oxide nanoparticles encapsulation within poly(d,l-lactide-co-glycolide) sub-micron particles. *Eur J Pharm Biopharm* 67: 31–38.
- Okuhata Y (1999) Delivery of diagnostic agents for magnetic resonance imaging. *Adv Drug Deliv Rev* 17: 31–48.
- Owen DE, Peppas NA (2006) Opsonization, biodistribution and pharmacokinetics of polymeric nanoparticles. *Int J Pharm* 307: 93–102.
- Popplewell J, Sakhini L (1995) The dependence of the physical and magnetic properties of magnetic fluids on particle size. *J Magn Mater* 149: 72–78.
- Park J, An K, Hwang K (2004) Ultra-large-scale syntheses of monodisperse nanocrystal. *Nat Mater* 3: 891–895.
- Seo WS, Lee JH, Sun XM, Suzuki Y, Mann D, Liu Z (2006) FeCo/graphitic-shell nanocrystals as advanced magnetic-resonance-imaging and near-infrared agents. *Nat Mater* 5: 971–976.
- Sonvico F, Mornet S, Vasseur S, Dubernet C, Jaillard D (2005) Folate-conjugated iron oxide nanoparticles for solid tumor targeting as potential specific magnetic hyperthermia mediators: synthesis, physicochemical characterization, and *in vitro* experiments. *Bioconjug Chem* 16: 1181–1188.
- Strable E, Bulte JWM, Moskowitz B (2001) Synthesis and characterization of soluble iron oxide-dendrimer. *Chem Mater* 13: 2201–2209.
- Tai LA, Tsai PJ, Wang YC, Wang YJ, Lo LW (2009) Thermosensitive liposomes entrapping iron oxide nanoparticles for controllable drug release. *Nanotechnology* 20: 135101–135110.
- Tapan KJ, Richey J, Strand M, Leslie-Pelecky DL (2008) Magnetic nanoparticles with dual functional properties: Drug delivery and magnetic resonance imaging. *Biomaterials* 29: 4012–4021.
- Talelli M, Rijcken CJ, Lammers T, Seevinck PR, Storm G (2009) Superparamagnetic iron oxide nanoparticles encapsulated in biodegradable thermosensitive polymeric micelles: toward a targeted nanomedicine suitable for image-guided drug delivery. *Langmuir* 25: 2060–2067.
- Tomita K, Tanimoto A, Irie R, Kikuchi M (2008) Evaluating the severity of nonalcoholic steatohepatitis with superparamagnetic iron oxide-enhanced magnetic resonance imaging. *J Magn Reson Imaging* 28: 1444–1450.

Xie J, Xu CJ, Kohler N (2007) Controlled PEGylation of monodisperse Fe_3O_4 nanoparticles for reduced non-specific uptake by macrophage cells. *Adv Mater* 19: 3163–3166.

Xiong F, Li J, Wang H, Chen YJ (2006) Synthesis, properties and application of a novel series of one-ended monooleate-modified poly(ethylene glycol) with active carboxylic terminal. *Polymer* 47: 6636–6641.

Yuan JJ, Armes SP, Takabayashi Y, Prassides K, Leite C, Galembeck F, Lewis AL (2006) Synthesis of biocompatible poly[2-(methacryloyloxy)ethyl phosphorylcholine]-coated magnetite nanoparticles. *Langmuir* 22: 10989–10993.

Win KW, Feng S (2005) Effects of particle size and surface coating on cellular uptake of polymeric nanoparticles for oral delivery of anticancer drugs. *Biomaterials* 26: 2713–2722.